Teleseismic constraints on horizontal sensor orientations of Hongseong geophone array

Min-Seong Seo[1] and Minkyung Kim[2]

[1] 36wnfgodfkd@snu.ac.kr, [2] shinyjade@snu.ac.kr

Hongseong geophone array (hereafter HS array) was deployed on the surface. Although it was installed considering the orientation, it is also important to check whether it is installed properly. It is challenging to apply widely used methods such as *P*-wave or Rayleigh-wave polarization-based methods due to small number of large ($M \geq 5.5$) events available during the relatively short period. Alternatively, we explored capability of utilizing full waveform traces of 12 well-recorded teleseismic events that occurred during the HS array deployment period.

The idea is that teleseismic events should show high coherency between their waveforms for the stations deployed close enough if filtered at very low frequency. The prerequisites are that (1) array aperture should be sufficiently small relative to the adopted frequency band, (2) signal-to-noise ratio should be sufficiently high, and (3) station with known orientation should exist in the vicinity of the array. 12 events listed in Table 1 satisfy the first two conditions at carefully chosen frequency band of 0.05 – 0.5 Hz. The broadband station HSB of KG network was located nearly of the HS array with the reported misorientation angle of 47.47°, during the deployment period (Son et al., 2021). If correctly oriented, the radial and transverse component records would show high correlation with those of HSB and otherwise, the degree of correlation would be lowered. Therefore, one can grid search for the relative angle that maximizes the average correlation coefficient of radial and transverse records (CC_{RT}) between the selected geophone and HSB station. We note that this method was successfully validated and applied by Grigoli et al. (2012) and Seo et al. (2022).

Since geophone sensors and broadband station HSB are not strictly collocated, time lag is first calculated from the cross-correlation of vertical components records. The estimated time lag is then used to align the horizontal component records of geophone sensors relative to those of HSB before calculating CC_{RT}. The correlation coefficients between the vertical component records are overall very high (>0.9), which validates the choice of frequency band. Teleseismic waveforms are cut from 20 s before to 80 s after the theoretical *P* wave arrival estimated with IASP91 for the analysis.

We applied the method to estimate the misorientation angles of 116 geophones, excluding 015P and 113P which were deployed at the period of the preliminary investigation and hence did not record any of 12 events. We then calculated the median absolute deviations (MAD) for each geophones, and the angles that deviated from the median by 3*MAD were treated as outliers and then excluded, and the circular mean was taken for the remaining angles. In most geophones, the similar misorientation angles

and small MAD values were calculated for all event, but the large MAD values were obtained for few stations. This seems to have been affected by the characteristics of the sites or noises, therefore, the misorientation angle of a geophone showing a large MAD value should be used with caution.

We can compare the waveforms before and after orientation correction in Figure 2 and Figure 3. We obtained the misorientation angle of 57.8°±3.615° for station 021H. The correction improves the correlation both the radial and the transverse components.

	latitude	longitude	depth	mag
2023-10-29T04:32:07.879Z	-19.3971	168.7776	72.481	6
2023-10-31T11:10:56.148Z	-17.5276	-179.01	550.172	6.5
2023-11-01T21:04:47.198Z	-10.0508	123.765	43	6.1
2023-11-08T04:52:51.393Z	-6.4442	129.7518	10	6.7
2023-11-08T04:53:50.283Z	-6.4194	129.5471	10	7.1
2023-11-08T13:02:06.115Z	-6.131	129.8738	10	6.7
2023-11-10T20:45:11.772Z	-6.0976	130.0606	9.969	6.1
2023-11-13T07:43:34.095Z	-3.8488	151.0831	10	6.1
2023-11-14T07:00:56.263Z	-4.0236	87.0994	10	6.1
2023-11-17T08:14:10.545Z	5.5711	124.9949	52	6.7
2023-11-22T02:48:51.641Z	1.7825	127.1884	102	6
2023-11-22T04:47:31.592Z	-14.9578	167.9708	13	6.7

Table 1. The list of 12 teleseismic earthquakes used for the analysis

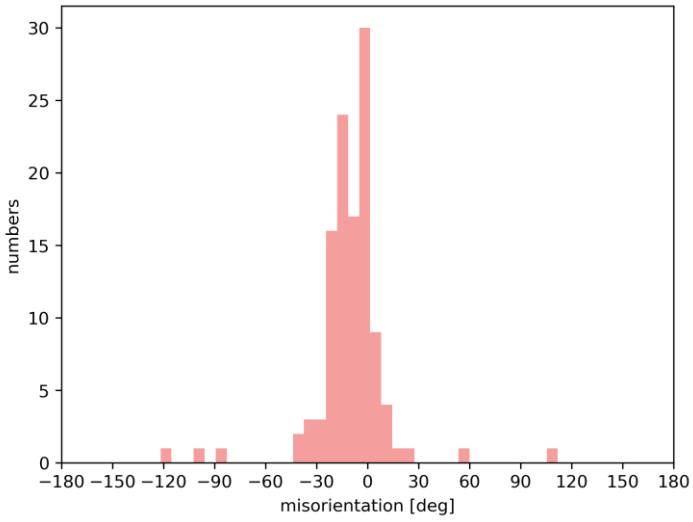

Figure 1. Histogram CC_{RT}-weighted estimates of misorientation angles.

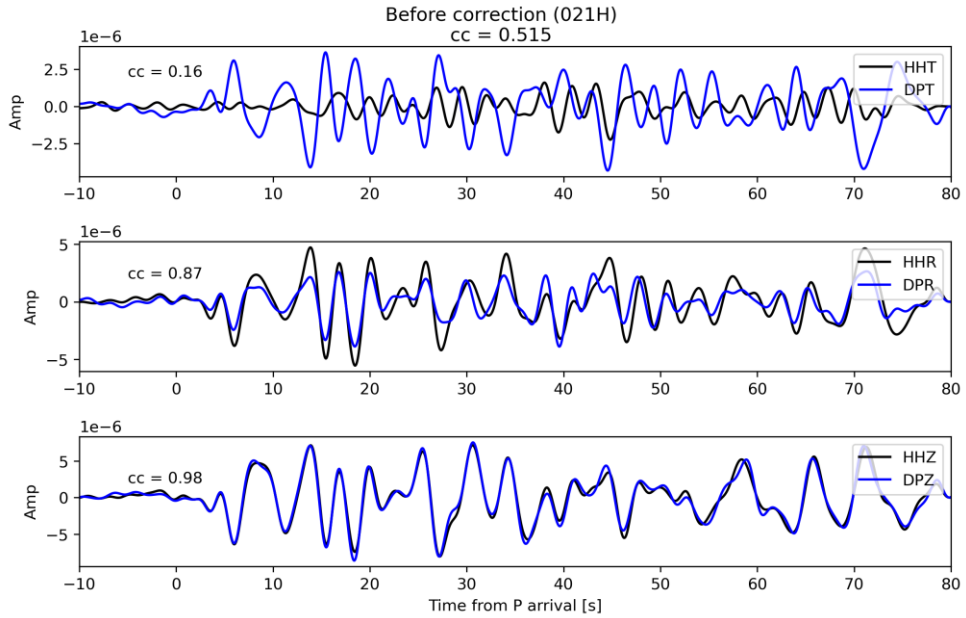

Figure 2. Comparison of bandpass-filtered (0.05 – 0.5 Hz) waveforms of event 2023-11-08 13:02:06 recorded at station 021H (blue) and HSB (black) before orientation correction. The correlation coefficients of each waveform are marked in the figure. The instrumental responses were removed, and the amplitudes were not normalized.

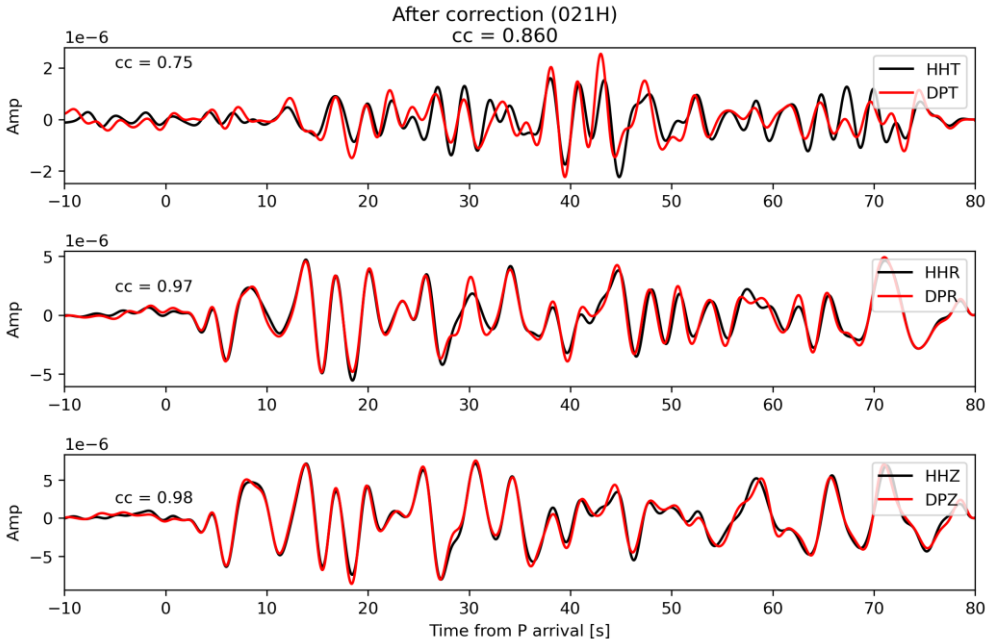

Figure 3. Comparison of bandpass-filtered (0.05 – 0.5 Hz) waveforms of event 2023-11-08 13:02:06 recorded at station 021H (red) and HSB (black) before orientation correction. The correlation coefficients of each waveform are marked in the figure. The instrumental responses were removed, and the amplitudes were not normalized.

References

Grigoli, F., Cesca, S., Dahm, T., & Krieger, L. (2012). A complex linear least-squares method to derive relative and absolute orientations of seismic sensors. *Geophysical Journal International*, *188*(3), 1243-1254.

Lee, S. J. (2021). Determining the Orientation of Accelerograph Stations in South Korea using Ambient Noise Data. *Journal of the Korean earth science society*, *42*(2), 195-200.

Seo, M. S., Son, Y. O., Kim, Y., Kang, T. S., Rhie, J., Kim, K. H., & Ree, J. H. (2022). Measurement of seismometer misorientation based on P-wave polarization: application to dense temporary broadband seismic array in the epicentral region of 2016 Gyeongju earthquake, South Korea. *Geosciences Journal*, *26*(3), 385-397.

Son, Y. O., Seo, M. S., & Kim, Y. (2021). Measurement of seismometer misorientation based on P-wave polarization: application to permanent seismic network in South Korea. *Geosciences Journal,* 1-13.